Published in *Proceedings of the International Symposium on Lightning Protection (XVII SIPDA)*, Suzhou, China, 9-13 october 2023, which should be cited to refer to this work.
DOI: 10.1109/SIPDA59763.2023.10349151

2023 International Symposium on Lightning Protection (XVII SIPDA), Suzhou, China, October 9-13, 2023

Full-Wave Analysis of Wind Turbine Transient Response to Direct Lightning Strikes

Riccardo Torchio
Dept. of Industrial Engineering
University of Padova
Padova, Italy
riccardo.torchio@unipd.it

Martino Nicora
ICT and Electrical Engineering Dept.
University of Genoa
Genoa, Italy
martino.nicora@edu.unige.it

Daniele Mestriner
ICT and Electrical Engineering Dept.
University of Genoa
Genoa, Italy
daniele.mestriner@unige.it

Massimo Brignone
ICT and Electrical Engineering Dept.
University of Genoa
Genoa, Italy
massimo.brignone@unige.it

Renato Procopio
ICT and Electrical Engineering Dept.
University of Genoa
Genoa, Italy
renato.procopio@unige.it

Piergiorgio Alotto
Dept. of Industrial Engineering
University of Padova
Padova, Italy
piergiorgio.alotto@unipd.it

Marcos Rubinstein
Institute for Information and Communication Technologies
University of Applied Sciences and Arts of Western Switzerland
Yverdon-les-Bains, Switzerland
marcos.rubinstein@heig-vd.ch

***Abstract*—Lightning strikes attachment to Wind Turbines (WTs) is not uncommon. The current discharge along the WT components can cause variations in the electromagnetic field radiation, affecting the surrounding power and electronic systems. In this contribution, a WT transient response to direct lightning strikes is studied with a full-Maxwell approach, involving a complete model for the WT. Simulations are carried out considering both first and subsequent return strokes to one of the rotor blades. Significant reflections are found in the lightning current waveforms through the WT, and this gives rise to amplifications in the radiated electromagnetic fields with respect to ground discharges.**

Keywords—Lightning, lightning electromagnetic pulse, return stroke current, lightning at tall structures, wind turbines.

I. Introduction

Lightning strikes represent an important source of risk for Wind Turbines (WTs) due to their exposure (tall objects in isolated locations) [1, 2], to the ever more common use of poor-conductivity carbon-fiber-reinforced polymers in the rotor blades [3] and to the triggering effect associated to blade rotation [3-5]. A considerable amount of direct lightning strikes can be experienced by WTs, and this implies damages, costs, and safety issues [6-8].

The main principles regarding lightning protection of WTs are provided in the standard IEC 61400-24 [9]. Each blade should be equipped with an air termination system aimed at attracting the lightning discharge. The current pulse propagates along the WT components (rotor blade, hub, nacelle, tower) by means of metal down-conductors and is discharged into the earth-termination system.

In this contribution, a full-wave analysis of direct lightning strikes to WTs is presented. The lightning current waveform in the channel and along the WT is computed and used to calculate the ElectroMagnetic (EM) fields.

It is known that the peak value and the maximum steepness of the EM fields radiated by lightning return strokes to a tall structure (at a distance greater than its height) may be 2-3 times greater compared with the same discharge to the ground [10, 11]. This can significantly affect the overvoltage induced on the surrounding power and electronic systems.

Moreover, an accurate lightning current evaluation in the WT is required to assess the potential distribution in components and design the appropriate protection system (surge protection devices, equipotential bonding) [12].

The rest of the paper is organized as follows. An overview on modelling approaches for lightning return strokes to tall objects is presented in Section II. The WT model and the full-wave method are the objects of Section III. Results are shown and discussed in Section IV. Finally, conclusions are presented in Section V.

II. Modelling Tall Objcects Struck by Lightning

Different studies on the WT transient response to direct lightning strikes are available in the literature. Most of these consist in simulations with the Electromagnetic Transients Program-Alternative Transient Program (EMTP-ATP) [12-14] and are based on the well-known Transmission Line (TL) modelling approach for lightning return strokes to tall objects [15-17].

The TL-based models consider two opposite current pulses injected at the interface point. The upward one propagates along the lightning channel at a certain return-stroke speed v (usually from $c_0/3$ to $c_0/2$, with c_0 the speed of light in vacuum). The downward one propagates with $v = c_0$ through the object, which is modelled as a lossless uniform TL. Such an approach implies the evaluation of constant reflection coefficients at the extremities of the structure and between its main components, that may be a difficult task when objects with considerable structural complexity are involved (i.e., WTs). This may lead to improper descriptions and inaccurate results.

An alternative approach is the one proposed by electromagnetic models (e.g., [18, 19]) where the object is treated as a wire structure and the lightning channel is assumed to be a lossy vertical wire antenna. A voltage source is placed in the channel-WT interface and Maxwell's equations are solved numerically, e.g., with the Method of Moments (MoM).

Thus, in this paper the WT response to direct lightning is modelled with a full-wave approach, through which it is possible to consider a detailed WT 3-D model, without any relevant assumption, except for channel verticality. A complete description is presented in the following section.

III. Lightning Strikes to WTs: Model and Method

A. 3-D Model

A horizontal axis WT with three blades is considered. The geometry and materials with their conductivities (σ) are reported in Table I. Fig. 1 shows the model of the WT struck by a lightning discharge. An internal down-conductor made of copper is wired inside the blades and is connected to the tower through the hub, providing a conductive path for the lightning current. The lightning-WT interface point is assumed to be at the top of a blade in the upward vertical position.

For the WT earthing system, the configuration proposed in [20], which is modelled with an equivalent π-circuit (Fig. 2), is assumed in a soil with σ =1 mS/m and ε_r =10. However, as done in other studies (e.g., [18, 19]), the ground is assumed to be a Perfect Electric Conductor (PEC) when the EM fields are computed. The lightning channel is represented with the model proposed in [21], i.e., a straight vertical cylindrical conductor with a diameter of 20 cm and an electrical resistivity of 70 mΩ/m.

This analysis is focused on the return stroke, which is the process giving rise to the main contribution to the lightning EM fields. Thus, the upward connecting leader, which commonly characterizes the lightning attachment to tall objects, is not considered. The possibility of neglecting this phenomenon has been assessed by means of preliminary simulations assuming a bidirectional return stroke model [22].

B. Numerical Method

The problem involves open boundary, fast transients for an electrically long structure (channel + WT) and structural details of the struck object. These complexities made us develop an appropriate Integral Equation Method (IEM), based on the Partial Element Equivalent Circuit (PEEC) method. Since transient analyses are performed, we chose a time-domain version of the PEEC method, built on the Marching On-In-Time (MOT) scheme [23, 24]. The developed MOT-PEEC method is based on the following set of equations [25]:

$$\mathbf{E}(\mathbf{r}, t) = -\partial\mathbf{A}(\mathbf{r}, t) / \partial t - \nabla\varphi(\mathbf{r}, t) + \mathbf{E}_{inc}(\mathbf{r}, t) \quad (1)$$

$$\mathbf{E}(\mathbf{r}, t) = \mathbf{J}(\mathbf{r}, t) / \sigma(\mathbf{r}) \quad (2)$$

$$\nabla\cdot\mathbf{J}(\mathbf{r}, t) = -\partial\rho(\mathbf{r}, t) / \partial t \quad (3)$$

TABLE I. WT model details

WT component	material	σ [S/m]	geometry
blades	GFRP[a]	10^{-2}	length 67 [m] thickness 50 [mm]
hub	cast iron	$2\cdot10^{6}$	diameter 6[m] thickness 100 [mm]
nacelle	GFRP	10^{-2}	length 20 [m] thickness 30 [mm]
tower	structural steel	$4\cdot10^{6}$	heigth 99 [m] thickness 30 [mm]
down-conductor	copper	$6\cdot10^{7}$	diameter 8 [mm][b]

[a.] Glass Fiber Reinforced Polymer
[b.] recommended in [9]

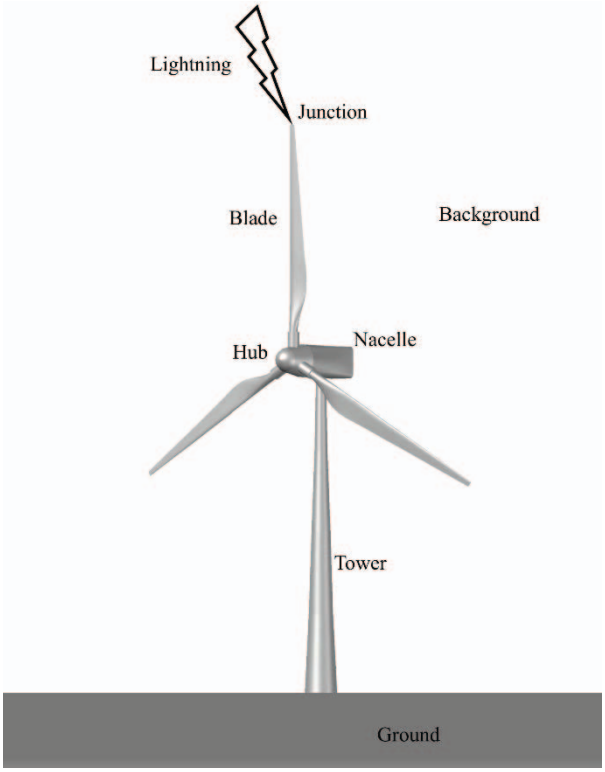

Fig. 1. WT representation. The downconductor passes inside the components

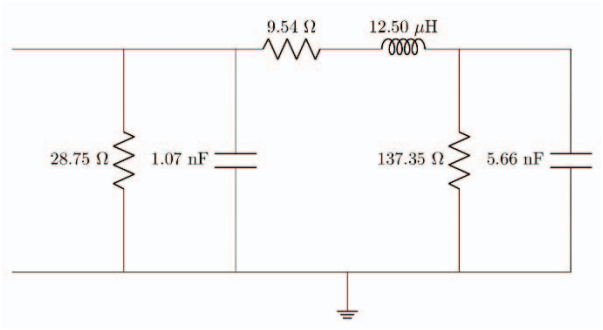

Fig. 2. Equivalent circuit of the WT earthing system.

where (1) is the Electric Field Integral Equation (EFIE), (2) is Ohm's law, and (3) is the continuity equation. **E** is the electric field, **r** is the observation point, **A** is the magnetic vector potential, φ is the scalar electric potential, $\mathbf{E}_{inc}$ is the incident electric field, **J** is the current density, ρ is the charge density and σ is the electric conductivity.

J and φ are selected as unknowns and approximated with shape functions, according to what is recommended in [24]. Then, space and time discretization is achieved by means on the Galarkin (collocation) method. The resulting MOT-PEEC equations are:

$$(\mathbf{R}+\mathbf{L}_0)\mathbf{j}^{(s)}+\frac{1}{2}\tilde{\mathbf{A}}^T\Phi^{(l)}=\mathbf{e}_{inc}^{(s)}-\sum_{u=1}^{H_T}(L_u\mathbf{j}^{(s-u)})-\frac{1}{2}\tilde{\mathbf{A}}^T\Phi^{(l-1)} \quad (4)$$

$$\mathbf{P}_0\tilde{\mathbf{A}}\mathbf{j}^{(s)}+\frac{1}{\Delta t}\Phi^{(l)}=-\sum_{u=1}^{H_T}(\mathbf{P}_u\tilde{\mathbf{A}}\mathbf{j}^{(s-u)})-\frac{1}{\Delta t}\Phi^{(l-1)} \quad (5)$$

where $\mathbf{R}$, $\mathbf{L}_k$ and $\mathbf{P}_k$ (k=0, …, H_T) are the MOT-PEEC matrices, (related to resistance, inductance, and potential terms, respectively); $\tilde{\mathbf{A}}$ is the incidence matrix of the equivalent circuit [25]; $\mathbf{j}$, Φ and $\mathbf{e}_{inc}$ are the discretization arrays of $\mathbf{J}$, φ and $\mathbf{E}_{inc}$, respectively. Superscripts refer to time instants and are such that $t_l - t_s = s\Delta t - l\Delta t = \Delta t / 2$ (where Δt is the time step). $H_T = \lceil 1+D_{max} / (\Delta t\ v) \rceil$ is the number of previous time steps affecting the solution of the present time instant, where $\lceil\cdot\rceil$ is the ceiling operator, D_{max} is the maximum distance between two element of the mesh, and $v = (\varepsilon_b\ \mu_b)^{-1/2}$ is the speed of light in the background medium (with ε_b and μ_b being its permittivity and permeability, respectively).

Inductance and potential matrices record the instantaneous and delayed interactions between the unknowns. The Green's function of the background is used to evaluate the elements of the matrices:

$$L_{u,kh}=\mu_b\int_{\Omega}\int_{\Omega'}\frac{\mathbf{w}_k(r)\cdot\mathbf{w}_h(r')\dfrac{\partial T(t_u')}{\partial t'}}{4\pi\|\mathbf{r}-\mathbf{r}'\|}d\Omega' d\Omega \quad (6)$$

where $\mathbf{w}$ is the space function of space, T is the space function of time, $\mathbf{r}'$ is the position of the source, $t' = t - \|\mathbf{r}-\mathbf{r}'\| / v$ is the delayed time, and $t_u' = u\Delta t - \|\mathbf{r}-\mathbf{r}'\| / v$ is its discrete version.

C. Assumptions

1) Return stroke speed: The lightning pulse propagates along the channel with a speed that is lower than c_0 (speed of light in vacuum). However, complex local phenomena, that depend on the current itself, make the exact evaluation of the return stroke speed (that in general is not constant) a difficult task [26]. In this framework, a constant return stroke speed is assumed according to what is proposed in [21], i.e., modelling the channel region with a fictitious medium of relative permittivity ε_r = 5.3 such that $v = (\varepsilon_r\ \varepsilon_0\ \mu_0)^{-1/2} = 1.3\cdot10^8$ m/s (ε_0 and μ_0 being the electric permittivity and magnetic permeability of vacuum, respectively). On the other hand, in the WT, the propagation speed of the lightning pulse is c_0. Therefore, the IEM is developed allowing different propagation modes in different regions of the model. Self and mutual coefficients of the WT matrices and the WT-channel mutual coefficients are computed imposing a background with vacuum permittivity and permeability, whereas those of the channel matrices account for ε_r = 5.3. Once the $\mathbf{J}$ distribution is obtained, the generated EM fields are computed with typical integral equations [10, 19, 21] choosing a background with vacuum parameters, since the EM fields propagation speed in vacuum is c_0.

2) Exitation source: Most TL-based models (e.g., [15, 16]) consider a current injection at the interface between the channel and the struck object, i.e., the Channel-Base Current (CBC). Typically, the Heidler function [27] or a combintion of two or more Heidler functions is assumed to rapresent the CBC. Then, the current distribution is evaluated analytically

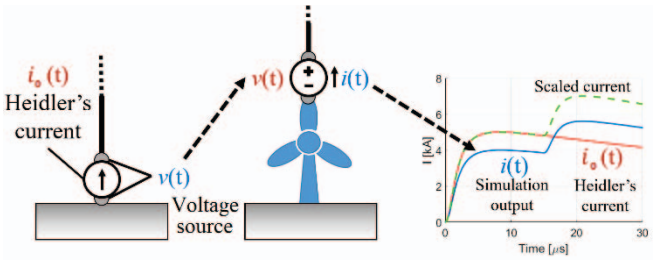

Fig. 3. Source modelling. Imposed quantity in red, computed quantity in blue.

superimposing the source effect with those of reflections. Clearly, results depend on the reliability of the imposed reflection coefficients (difficult evaluation when complex structures are studied).

On the other hand, in full-wave models, it is not possible to assume the CBC source at the interface with the WT since it would suppress reflection effects. Thus, the phenomenon is assumed to be voltage-driven and an ad-hoc voltage source is selected. The workflow of the proposed approach (depicted in Fig. 3) is the following.

- A first simulation is performed with a ground-initiated return stroke in which the CBC is imposed as the source of the problem (i.e., assuming Heidler's expression for the CBC).
- The voltage $v(t)$ across the current source is computed and is assumed as the source of a new simulation in which both the WT and the lightning channel are present.
- The current $i(t)$ at the junction between the WT and channel is computed.
- The voltage source is scaled so that such current before the occurrence of the first reflection coincides with the Heidler's CBC.

3) Skin effect: In principle, the skin depth variations in the metallic structure of the WT during propagation may affect the results. To assess this issue, preliminary simulations are performed following the approach of [28], leading to comparable results (in terms of current distribution and radiated EM fields) when the skin depth variation is considered and when all the WT components are assumed as PEC. This is because in the considered system, the elements of the MOT-PEEC resistance matrix (that are associated with the skin depth) are significantly lower than those of the inductance matrices. Therefore, the WT components are assumed as PEC.

IV. Results

This section presents the lightning current evolution in the channel and in the WT and the radiated EM fields. Both first and subsequent return strokes are considered, assuming the Heidler's function [27] parameters for the CBC that are reported in [10]. Thus, two different voltage sources have been computed according to the approach described in the previous section. Results are compared with ground-initiated discharges (i.e., removing the WT and directly imposing the Heidler's current at ground level).

A. Current ditributions

Fig. 4 shows the current distributions when a first return stroke is considered. Panel (a) reports the current waveform

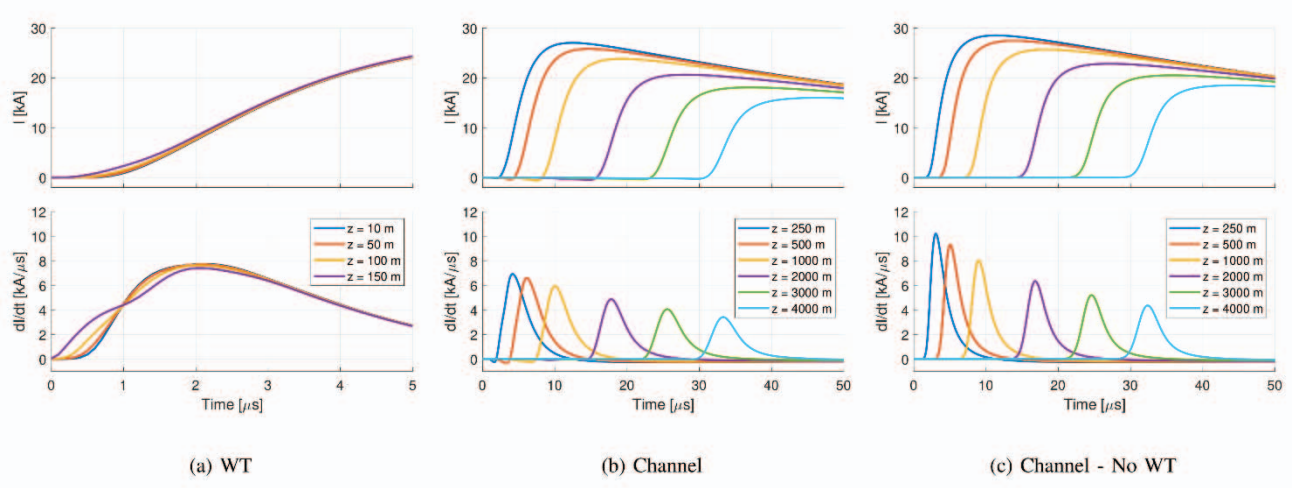

Fig. 4. First return stoke current and current derivative waveforms along the WT and along the lightning channel

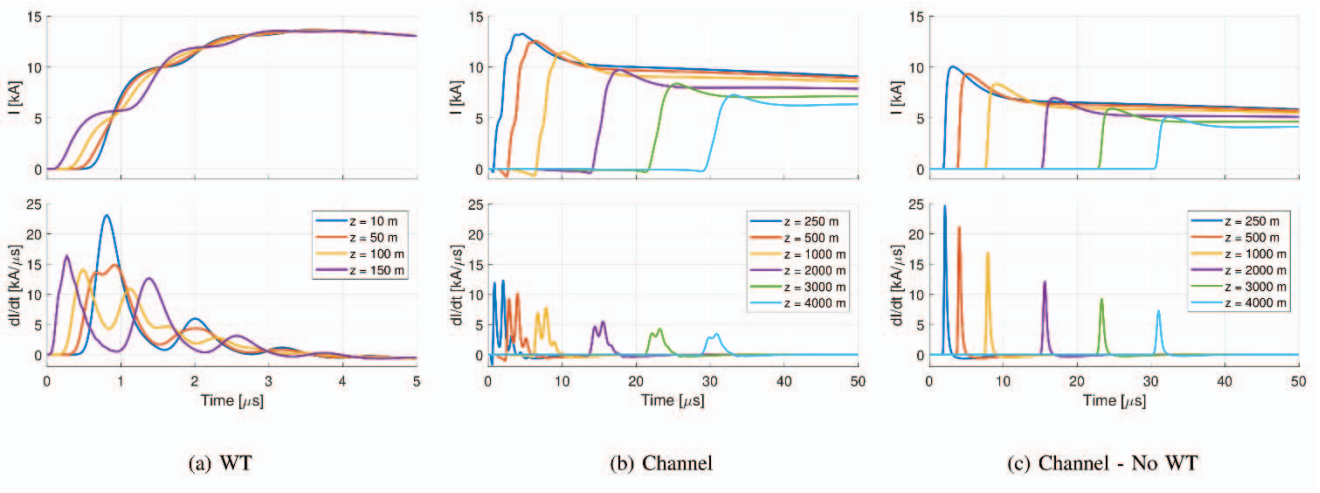

Fig. 5. Subsequent return stoke current and current derivative waveforms along the WT and along the lightning channel .

and its derivative along the WT in a time window of 5 μs (after that, no significant dynamics are recorded). It is worth noting that they are observed only along the vertical direction at different heights z from the ground (the total height of the structure is 172 m), although the current path has other (minor) directions (e.g., along the nacelle). Reflections that occur at the top and at the bottom of the WT are not discernible because the WT is electrically short for the first return stroke risetime. Hence, for the frequency spectrum of first return strokes, this result may allow TL-based models to approximate the WT with a lumped impedance. A slight current distortion can be noticed by observing the derivative waveforms, whereas current attenuation along the WT is almost negligible, due to its relatively short length.

Panels (b) and (c) show the current waveform and its derivative along the channel for WT-initiated and ground-initiated return strokes, respectively. Attenuation and distortion phenomena can be observed, in agreement to what is reported in [21]. It can be noticed that the distortion is more significant when the WT is not present. Indeed, the decrease of the derivate peak from 250 m to 4000 m is 50% in panel (b) and 58% in panel (c). On the other hand, the current attenuation in the channel is more pronounced when the WT is present, i.e., the reduction of the current peak from 250 m to 4000 m is 40% in panel (b), 35% in panel (c). These differences may be due to the WT-channel mutual coupling. It is interesting to observe that the current waveforms of panel (b) exhibit a negative undershoot in the first part of the propagation process. This phenomenon is produced by the negative current induced in the channel by the fields radiated by the downward current pulse propagating along the WT at c_0. The current starts increasing and becomes positive when the upward current pulse propagating along the channel at $v = 1.3 \cdot 10^8 < c_0$ reaches the observation point. Indeed, this effect is not present in panel (c), where the WT is not considered.

Fig. 5 shows the current distributions when a subsequent return stroke is considered. Here, it is possible to discern multiple reflections. With reference to the current derivative waveform along the WT observed at 100 m and represented with the ochre line in panel (a), the first ground reflection appears at 0.90 μs; successively, a reflection related to the channel interface is present at 1.37 μs; then, they follow subsequent reflections associated with discontinuities both at the bottom and at the top of the WT. Thus, for the frequency spectrum of subsequent return strokes, this result suggests that the TL-based model should consider the discontinuity related to the WT-channel interface.

Current distortion on the WT can be observed in the derivative waveform of panel (a), where a peak reduction is present in the time interval before the arrival of arrival of the

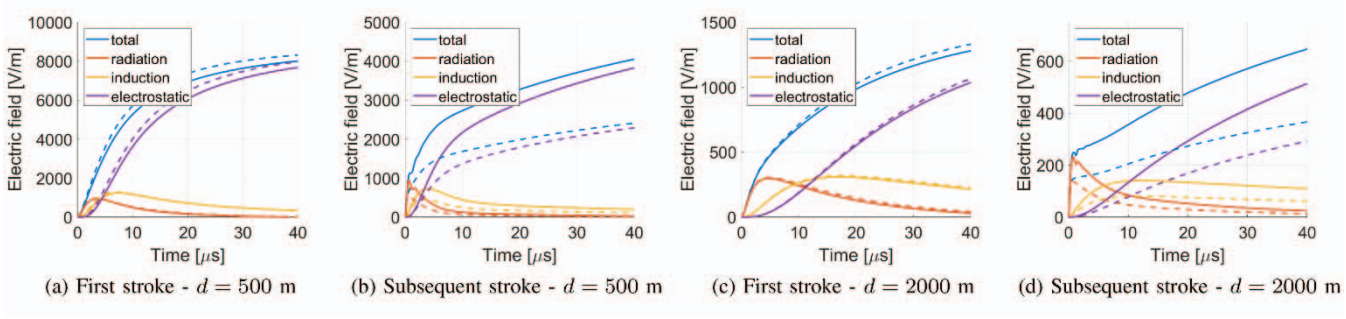

Fig. 6. Vertical E-field at ground at two distances d from WT-initiated (solid lines) and ground-initiated (dashed lines) first and subsequent return strokes

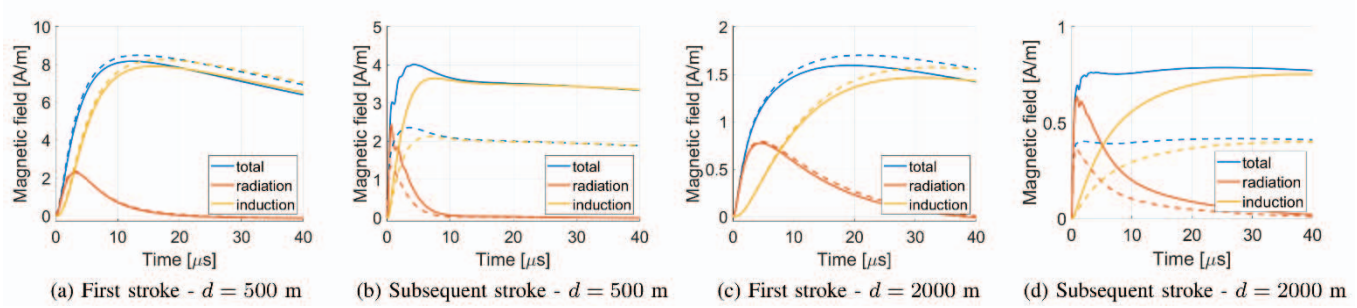

Fig. 7. Azimuthal H-field at ground at two distances d from WT-initiated (solid lines) and ground-initiated (dashed lines) first and subsequent return strokes.

first reflection. The upward and the downward current pulse along the WT show a comparable (slight) attenuation, in accordance with what is reported in [29] for the mechanism of current propagation along conical structures with base radius much lower than height. Also, in the subsequent return stroke case, distortion and attenuation characterize the current propagation along the channel both with and without the WT, as shown in panels (b) and (c), respectively. Nevertheless, differently from what has been found for the first return stroke case, propagation modes with and without the WT are comparable.

B. EM fields

The EM fields are observed at ground level and at two horizontal distances from the source, i.e., 500 m and 2000 m. In Fig. 6 (Fig. 7), the static, induction, and radiation terms of the vertical electric field (induction and radiation terms of the azimuthal magnetic field) are displayed separately for both first and subsequent return strokes. Solid lines are related to WT-initiated return strokes, whereas dashed lines are related to ground-initiated return strokes.

Static, radiation and induction contributions to the overall fields depend on the distance from the source. The more the observation point is far from the source, the more the effect of radiation is dominant [18, 19]. This trend is consistent with the computed EM fields at 500 m and 2000 m (Figs. 6 -7).

The current waveform of subsequent return strokes has a lower time-to-peak and higher maximum steepness than that of the first return stroke. Thus, the radiation term (that is associated with the initial rising ramp) is more relevant for the subsequent return stroke EM fields. Comparing solid lines (EM fields with the WT) and dashed lines (EM fields without the WT), it can be concluded that, for the first return stroke case, no enhancements are produced by the presence of the WT (i.e., when the WT is considered, slightly lower values are obtained due to the effect of the earthing system). On the other hand, subsequent return stroke EM fields show a 1.7-1.8 amplification factor when the WT is considered.

Moreover, the waveforms of WT-initiated return stroke EM fields are affected by oscillations (mainly in the radiation term) that are associated with current reflections in the WT. When the first return stroke case is considered, the maximum steepness of EM fields is comparable with and without the presence of the WT (both at 500 m and 2000 m, both for the E-field and the H-field). In contrast, for subsequent return stroke EM fields, the maximum steepness increases by a factor 1.7-1.8 when the initiation occurs at the WT.

C. Other results

A sensitivity analysis is performed on some parameters and is briefly discussed in the following (graphical results are omitted for the sake of brevity). Only the subsequent return stroke case is considered since only minor effects are detected for the first return stroke case.

1) Relation between the structure height and the current time-to-peak: Assuming the same CBC parameters (from which the approriate voltage source is computed), a scaled-up WT with total height of 268 m (compared to the 172 m total height of the WT considered previously) is considered. Simulations have revealed no relevant changes in the EM fields with respect to the previous scenario. This is in good agreement with the observations of [30], i.e., when $2h/c_0$ (where h is the tall struck object height) is grater the current time-to-peak, the EM fields amplification factor does not depend on h, but only on v, c_0, and on the top and bottom reflection coefficients.

2) Effects associated with the rotation angle of the struck blade: Simulations are repeated assuming the struck blade rotated by 60° with respect to the upward vertical position. Analogous results in terms of current distribution are obtained (both in the WT and in the channel). The EM fields at 500 m increase by a factor 1.1-1.3 when the

inclined struck blade is considered, whereas no variations appear for the EM fields at 2000 m.

V. Conclusion

This contribution has presented a full-wave analysis of the Wind Turbine (WT) transient response to direct lightning strikes. An integral equation method based on the partial element equivalent circuit scheme has been developed in the time-domain. A detailed 3-D model of the WT has been considered. The lightning pulse has been modelled as a voltage source placed between the WT and the lightning channel. For both first and subsequent return strokes, the obtained current distributions along the channel exhibit relevant attenuation and distortion phenomena comparable with those of ground-initiated lightning. When a first return stroke is considered, reflections that occur at the top and at the bottom of the WT are not discernible since the WT is electrically short in this case, whereas multiple discernible reflections characterize the propagation of the subsequent return stroke current. Lightning EM fields generated by a first return stroke are similar both with and without the presence of the WT. On the other hand, due to current reflections, subsequent return stroke EM fields increase by a factor 1.7-1.8 in magnitude and in maximum steepness when the initiation at the WT is considered. Future works will investigate the possibility of including a more accurate ground model with frequency-dependent electrical parameters.

Acknowledgment

The authors gratefully acknowledge the important and insightful comments and suggestions provided by Prof. Farhad Rachidi, which were instrumental in enhancing the quality of the paper.

.

References

[1] F. Rachidi, M. Rubinstein, and A. Smorgonskiy, "Lightning Protection of Large Wind-Turbine Blades," 2012, pp. 227-241.

[2] R. Alipio, D. Conceição, A. De Conti, K. Yamamoto, R. N. Dias, and S. Visacro, "A comprehensive analysis of the effect of frequency-dependent soil electrical parameters on the lightning response of wind-turbine grounding systems," *Electric Power Systems Research,* vol. 175, p. 105927, 2019/10/01/ 2019.

[3] F. Rachidi *et al.*, "A Review of Current Issues in Lightning Protection of New-Generation Wind-Turbine Blades," *IEEE Transactions on Industrial Electronics,* vol. 55, no. 6, pp. 2489-2496, 2008.

[4] J. Montanyà, O. van der Velde, and E. R. Williams, "Lightning discharges produced by wind turbines," *Journal of Geophysical Research: Atmospheres,* https://doi.org/10.1002/2013JD020225 vol. 119, no. 3, pp. 1455-1462, 2014/02/16 2014.

[5] Y. Wang *et al.*, "Influence of blade rotation on the lightning stroke characteristic of a wind turbine," *Wind Energy,* https://doi.org/10.1002/we.2341 vol. 22, no. 8, pp. 1071-1085, 2019/08/01 2019.

[6] K. Yamamoto, T. Noda, S. Yokoyama, and A. Ametani, "Experimental and analytical studies of lightning overvoltages in wind turbine generator systems," *Electric Power Systems Research,* vol. 79, no. 3, pp. 436-442, 2009/03/01/ 2009.

[7] S. Yokoyama, "Lightning protection of wind turbine blades," *Electric Power Systems Research,* vol. 94, pp. 3-9, 2013/01/01/ 2013.

[8] A. C. Garolera, S. F. Madsen, M. Nissim, J. D. Myers, and J. Holboell, "Lightning Damage to Wind Turbine Blades From Wind Farms in the U.S," *IEEE Transactions on Power Delivery,* vol. 31, no. 3, pp. 1043-1049, 2016.

[9] "Wind Turbine Generator Systems—Part 24: Lightning Protection," *IEC 61400-24,* 2019.

[10] F. Rachidi *et al.*, "Current and electromagnetic field associated with lightning-return strokes to tall towers," *IEEE Transactions on Electromagnetic Compatibility,* vol. 43, no. 3, pp. 356-367, 2001.

[11] Y. Baba and V. A. Rakov, "Lightning electromagnetic environment in the presence of a tall grounded strike object," *Journal of Geophysical Research: Atmospheres,* https://doi.org/10.1029/2004JD005505 vol. 110, no. D9, 2005/05/16 2005.

[12] J. Birkl, E. Shulzhenko, J. Kolb, and M. Rock, "Approach for evaluation of lightning current distribution on wind turbine with numerical model," in *2016 33rd International Conference on Lightning Protection (ICLP)*, 2016, pp. 1-8.

[13] N. Malcolm and R. Aggarwal, "Analysis of transient overvoltage phenomena due to direct lightning strikes on wind turbine blade," in *2014 IEEE PES General Meeting | Conference & Exposition*, 2014, pp. 1-5.

[14] L. Zhang, S. Fang, G. Wang, T. Zhao, and L. Zou, "Studies on an Electromagnetic Transient Model of Offshore Wind Turbines and Lightning Transient Overvoltage Considering Lightning Channel Wave Impedance," *Energies*, vol. 10, no. 12. doi: 10.3390/en10121995

[15] F. Rachidi, V. A. Rakov, C. A. Nucci, and J. L. Bermudez, "Effect of vertically extended strike object on the distribution of current along the lightning channel," *Journal of Geophysical Research: Atmospheres,* https://doi.org/10.1029/2002JD002119 vol. 107, no. D23, pp. ACL 16-1-ACL 16-6, 2002/12/16 2002.

[16] J. L. Bermudez, M. Rubinstein, F. Rachidi, F. Heidler, and M. Paolone, "Determination of reflection coefficients at the top and bottom of elevated strike objects struck by lightning," *Journal of Geophysical Research: Atmospheres,* https://doi.org/10.1029/2002JD002973 vol. 108, no. D14, 2003/07/27 2003.

[17] Y. Baba and V. A. Rakov, "On the use of lumped sources in lightning return stroke models," *Journal of Geophysical Research: Atmospheres,* https://doi.org/10.1029/2004JD005202 vol. 110, no. D3, 2005/02/16 2005.

[18] Y. Baba and M. Ishii, "Numerical electromagnetic field analysis of lightning current in tall structures," *IEEE Transactions on Power Delivery,* vol. 16, no. 2, pp. 324-328, 2001.

[19] B. Kordi, R. Moini, W. Janischewskyj, A. M. Hussein, V. O. Shostak, and V. A. Rakov, "Application of the antenna theory model to a tall tower struck by lightning," *Journal of Geophysical Research: Atmospheres,* https://doi.org/10.1029/2003JD003398 vol. 108, no. D17, 2003/09/16 2003.

[20] F. M. Gatta, A. Geri, S. Lauria, and M. Maccioni, "Generalized pi-circuit tower grounding model for direct lightning response simulation," *Electric Power Systems Research,* vol. 116, pp. 330-337, 2014/11/01/ 2014.

[21] R. Moini, B. Kordi, G. Z. Rafi, and V. A. Rakov, "A new lightning return stroke model based on antenna theory," *Journal of Geophysical Research: Atmospheres,* https://doi.org/10.1029/2000JD900541 vol. 105, no. D24, pp. 29693-29702, 2000/12/27 2000.

[22] J. C. Willett, J. C. Bailey, V. P. Idone, A. Eybert-Berard, and L. Barret, "Submicrosecond intercomparison of radiation fields and currents in triggered lightning return strokes based on the transmission-line model," *Journal of Geophysical Research: Atmospheres,* https://doi.org/10.1029/JD094iD11p13275 vol. 94, no. D11, pp. 13275-13286, 1989/09/30 1989.

[23] C. Gianfagna, L. Lombardi, and G. Antonini, "Marching-on-in-time solution of delayed PEEC models of conductive and dielectric objects," *IET Microwaves, Antennas & Propagation,* https://doi.org/10.1049/iet-map.2018.5233 vol. 13, no. 1, pp. 42-47, 2019/01/01 2019.

[24] R. Torchio, D. Voltolina, P. Bettini, F. Moro, and P. Alotto, "Marching On-In-Time Unstructured PEEC Method for Electrically Large Structures with Conductive, Dielectric, and Magnetic Media," *Electronics*, vol. 9, no. 2. doi: 10.3390/electronics9020242

[25] R. Torchio, "A Volume PEEC Formulation Based on the Cell Method for Electromagnetic Problems From Low to High Frequency," *IEEE Transactions on Antennas and Propagation,* vol. 67, no. 12, pp. 7452-7465, 2019.

[26] V. Rakov, "Lightning Return Stroke Speed," *Journal of Lightning Research,* vol. 1, 01/01 2007.

[27] H. Heidler, "Analytische blitzstromfunktion zur LEMP-berechnung," in *18th ICLP*, Munich, Germany, 1985.

[28] M. Magdowski, S. Kochetov, and M. Leone, "Modeling the skin effect in the time domain for the simulation of circuit interconnects," in *2008 International Symposium on Electromagnetic Compatibility - EMC Europe*, 2008, pp. 1-6.

[29] A. Shoory *et al.*, "On the Mechanism of Current Pulse Propagation Along Conical Structures: Application to Tall Towers Struck by Lightning," *IEEE Transactions on Electromagnetic Compatibility,* vol. 54, no. 2, pp. 332-342, 2012.

[30] J. L. Bermudez *et al.*, "Far-field-current relationship based on the TL model for lightning return strokes to elevated strike objects," *IEEE Transactions on Electromagnetic Compatibility,* vol. 47, no. 1, pp. 146-159, 2005.